Standard and Regional Bio-Optical Algorithms for Chlorophyll a Estimates in the Atlantic off the Southwestern Iberian Peninsula

Sónia Cristina, Davide D'Alimonte, Priscila Costa Goela, Tamito Kajiyama, John Icely, Gerald Moore, Bruno Fragoso, and Alice Newton

***Abstract*—This study investigates standard and regional algal pigment index 1 (API1) estimates in the Atlantic off the southwestern Iberian Peninsula. Standard API1 data are those delivered by the Medium Resolution Imaging Spectrometer (MERIS) orbiting sensor. Equivalent quantities are computed by applying a regional inversion scheme using as input both MERIS and *in situ* remote sensing reflectances (R_{rs}). Reference data for the development of the regional algorithm and for the analysis of tested products include field measurements of total concentration of chlorophyll a (TChl*a*) and coincident R_{rs} values collected at different distances from the coast. Validation results, based on matchup analysis, identifies a systematic overestimation of standard API1 *versus* the reference TChl*a* values. The additional comparison of product maps in selected regions of interest confirms this tendency and demonstrates the feasibility and relevance of using regional algorithms for investigating spaceborne products. Analogous applications are hence devised for the early-stage evaluation of the forthcoming Sentinel-3/OLCI data products.**

***Index Terms*—Medium Resolution Imaging Spectrometer (MERIS) algal pigment index 1 (API1), multilayer perceptron (MLP) neural nets, ocean color, remote sensing reflectance.**

I. Introduction

THE long-term validation of data products delivered by the Sentinel missions of the European Space Agency (ESA) is required to meet performance targets for environmental studies (e.g., Copernicus program [1], [2]). Aware of the importance to assess and improve results in optically complex coastal waters, the present letter evaluates the algal pigment index 1 (API1) product from the Medium Resolution Imaging Spectrometer (MERIS) that operated from 2002 until 2012 onboard the ESA Envisat satellite. This product is related to equivalent results computed with regional bio-optical algorithms.

The standard API1 algorithm is a measure of the total concentration of chlorophyll a (TChl*a*), and it was developed for case 1 waters [3]. This study focuses on the comparison between the standard and regional bio-optical algorithms with *in situ* TChl*a*, (referred to as TChla^{REF}). The bio-optical regional products are computed with a multilayer perceptron (MLP) neural network [4]. In addition, the comparison between the standard MERIS API1 and the regional products is performed in selected regions of interests (ROIs) to derive cost-effective information complementing the direct matchup analysis. The two methods are evaluated in view of supporting investigations of the current and the new reprocessing of MERIS data products. This study is also strategic in establishing an operational framework for the timely evaluation of any product maps that may be provided in the future by the Ocean Land Colour Instrument (OLCI) onboard the Sentinel-3 spacecraft.

The investigated area is located off Sagres on the southwestern Iberian Peninsula, and it has been one of the MERIS validation sites since 2008. Field measurements were taken at three stations at 2, 10, and 18 km from the coast (stations A, B, and C, respectively) to cover waters affected by near-shore adjacency effects and those exposed by more offshore oceanic conditions. The Sagres coastal area is characterized by a narrow continental shelf and by an absence of permanent rivers. Upwelling events here are the main source of nutrients [5]. The sampling features of this site hence complement those of the other validation areas such as the Acqua Alta Oceanographic Tower (AAOT) in the Adriatic Sea [6] and the Bouée pour l'acquisition de Séries Optiques à Long Terme (BOUSSOLE) [7].

Manuscript received December 9, 2015; revised February 3, 2016; accepted February 3, 2016. Date of publication May 3, 2016; date of current version May 19, 2016. This work was supported in part by the European Space Agency (ESA) for the "Technical Assistance for the Validation of MERIS Marine Products at Portuguese oceanic and coastal sites" (contract no. 21464/08/I-O) and "MERIS validation and algorithm 4th reprocessing" (contract no. ARG/003-025/14067Sagremarisco and ARG/003-025/1406/CIMA). The works of S. Cristina and P. C. Goela were supported by Ph.D. Grants from the Portuguese FCT (SFRH/BD/78354/2011 and SFRH/BD/78356/2011, respectively). The work of A. Newton was supported by EU FP7 project DEVOTES (Grant no. 308392). The work of J. Icely was supported by EU FP7 AQUAUSER (Grant no. 607325) and Horizon 2020 AquaSpace (Grant no. 633476).

S. Cristina and P. C. Goela are with the Centre for Marine and Environmental Research (CIMA), University of Algarve, 8005-139 Faro, Portugal, and also with the Faculty of Marine and Environmental Sciences, University of Cadiz, 11510 Puerto Real, Spain (e-mail: cristina.scv@gmail.com; priscila.goela@gmail.com).

D. D'Alimonte is with the Centre for Marine and Environmental Research (CIMA), University of Algarve, 8005-139 Faro, Portugal (e-mail: davide.dalimonte@gmail.com).

T. Kajiyama is with the University of Algarve, 8005-139 Faro, Portugal (e-mail: rd6t-kjym@asahi-net.or.jp).

J. Icely and B. Fragoso are with the Centre for Marine and Environmental Research (CIMA), University of Algarve, 8005-139 Faro, Portugal, and also with Sagremarisco Lda., 8650-999 Vila do Bispo, Portugal (e-mail: john.icely@gmail.com; fragoso.b@gmail.com).

G. Moore is with the Crofters, Bio-Optika, Gunnislake PL18 9NQ, U.K. (e-mail: geraldfmoore@gmail.com).

A. Newton is with NILU-IMPEC, 2027 Kjeller, Norway, and also with the Centre for Marine and Environmental Research (CIMA), University of Algarve, 8005-139 Faro, Portugal (e-mail: an@nilu.no).

Color versions of one or more of the figures in this paper are available online at http://ieeexplore.ieee.org.

Digital Object Identifier 10.1109/LGRS.2016.2529182

II. Data and Methods

Radiometric measurements and water samples were collected between 2008 and 2012 at the three stations. The *in situ* radiometric measurements were used to calculate the normalized water-leaving reflectances (ρ_N) and were acquired with a tethered attenuation coefficient chain sensor (TACCS) manufactured by Satlantic; the processing details are reported in published studies [8] and [9]. The MERIS products selected for the matchup analysis and for the product map comparison were extracted, respectively, from the MERIS Level 2 Full Resolution (FR, 290 m $\times$ 260 m) and Reduced Resolution (RR, 1.2 km $\times$ 1.04 km) satellite images and analyzed with the Basic ERS & Envisat (A) ATSR and MERIS Toolbox (BEAM version 4.9). The retrieval of level 2 data was performed with the standard MEGS processor 8.1 (MERIS third reprocessing). The extraction procedure of the MERIS Level 2 products and the criteria for the matchup selection are presented in [9] and [10].

A. In Situ Total Chlorophyll a Reference Data

The *in situ* reference quantity for data product comparison, denoted as TChla^{REF}, was determined by high-performance liquid chromatography using Wright and Jeffrey methodology [11]. A detail description of the methodological steps is reported in [12].

B. Data Products Equivalent to TChla

1) MERIS Standard API1: The standard MERIS data product API1 (henceforth also referred to as MER$^{\mathrm{API1}}$) is the TChl*a* determined through a polynomial regression based on multiple band ratios of MERIS ρ_N [3]. TChl*a* comprises the sum of monovinyl chlorophyll a, divinyl chlorophyll a, chlorophyllide a, phaeophytin a, and phaeophorbide a.

2) Regional TChla Products: The regional TChl*a* products were computed using inversion schemes based on the MLP neural net. Results are derived from the *in situ* $R_{\mathrm{rs}}^{\mathrm{SITU}}$ and from the MERIS bottom-of-atmosphere $R_{\mathrm{rs}}^{\mathrm{MER}}$ remote sensing reflectance datasets (note that ρ_N is equivalent to R_{rs} upon scaling by π, i.e., $R_{\mathrm{rs}} = \rho_N/\pi$). Corresponding data products are henceforth denoted MLP($R_{\mathrm{rs}}^{\mathrm{SITU}}$) and MLP($R_{\mathrm{rs}}^{\mathrm{MER}}$), respectively. The applicability range of the regional algorithm was evaluated through a novelty detection scheme [13], [14]. This approach has already been used in former investigations to filter MLP inputs [15], [16] by assessing how well the input is represented within the MLP training dataset [15]. The MLP applicability range adopted here is based on a novelty index η computed from the principal component analysis [13] of log-transformed R_{rs} values. The key features of this novelty index are the following: 1) η is bounded between 0 and ∞; 2) the more the R_{rs} spectrum is similar to the *in situ* measurements used for training the regional MLP, the lower is its novelty index η; 3) an R_{rs} spectrum is considered within the MLP applicability range when η is below a threshold; and 4) independent analyses have shown that a threshold $\eta = 3$ fits the requirements for general application [13]. Different sets of center wavelengths (413, 443, 490, 510, 560, and 665 nm) were tested to derive the regional TChl*a* concentrations from spaceborne R_{rs}.

III. Results

Study results include both the analysis of matchup data and the comparison of product maps. For the matchup analysis, the following quantities are compared with the *in situ* TChl*a*: 1) MER$^{\mathrm{API1}}$; 2) MLP($R_{\mathrm{rs}}^{\mathrm{MER}}$); and 3) MLP($R_{\mathrm{rs}}^{\mathrm{SITU}}$). Data products were evaluated through the scattering and the bias as absolute (ε) and signed (δ) biased percent differences, respectively

$$\varepsilon = \frac{1}{N}\sum_{i=1}^{N}\frac{|y_i - x_i|}{x_i} \times 100;\ \ \delta = \frac{1}{N}\sum_{i=1}^{N}\frac{y_i - x_i}{x_i} \times 100 \tag{1}$$

where y_i indicates one of the tested products, x_i is the *in situ* reference, i is the sample index, and N is the number of samples. The coefficient of determination r^2 is also reported.

In addition to the matchup analysis, MER$^{\mathrm{API1}}$ and the MLP($R_{\mathrm{rs}}^{\mathrm{MER}}$) product maps were compared. These results are evaluated through the absolute (ε^*) and signed (δ^*) unbiased percent differences

$$\varepsilon^* = \frac{1}{N}\sum_{i=1}^{N}\frac{|y_i - x_i|}{y_i + x_i} \times 200;\ \delta^* = \frac{1}{N}\sum_{i=1}^{N}\frac{y_i - x_i}{y_i + x_i} \times 200 \tag{2}$$

where y_i and x_i are the MER$^{\mathrm{API1}}$ and MLP($R_{\mathrm{rs}}^{\mathrm{MER}}$) values, respectively, taking the mean of the two values as a reference.

Different sets of input wavelengths have been considered for testing the MLP performance. The set of R_{rs} at 490, 510, and 560 nm was selected as the MLP input by considering both the quality and the applicability range of regional data products in the study area. The MLP parameters for the Sagres region and the full set of functions for their operational application (including the definition of the applicability range) are available for download from http://ocportugal.org/sites/default/files/mlpSgr.pdf.

A. Matchup Data Analysis

The matchup results presented in Fig. 1 and Table I indicate that, of the tested products, MLP($R_{\mathrm{rs}}^{\mathrm{SITU}}$) has the best agreement with TChla^{REF}. The corresponding statistical figures are the following: scattering $\varepsilon = 29\%$, bias $\delta = 1\%$, and coefficient of determination $r^2 = 0.73$. The reported δ values for the three stations indicate an overestimate of MER$^{\mathrm{API1}}$, MLP($R_{\mathrm{rs}}^{\mathrm{MER}}$), and MLP($R_{\mathrm{rs}}^{\mathrm{SITU}}$) with respect to TChl$a^{\mathrm{REF}}$.

Table I also shows the scattering and bias associated with each sampling station; the largest uncertainties correspond to MER$^{\mathrm{API1}}$. The results from the standard and tested products are less accurate at station A but improve at station B and station C. For the MER$^{\mathrm{API1}}$ and the MLP($R_{\mathrm{rs}}^{\mathrm{MER}}$) products, this result suggests the presence of adjacency effects and possibly limitations in the aerosol models near the coast. However, in the case of the MLP($R_{\mathrm{rs}}^{\mathrm{SITU}}$), which only uses *in situ* radiometric data, there is also a degradation in the accuracy of the data product, possibly due to increasing complexity in the optical properties of seawater near the coast.

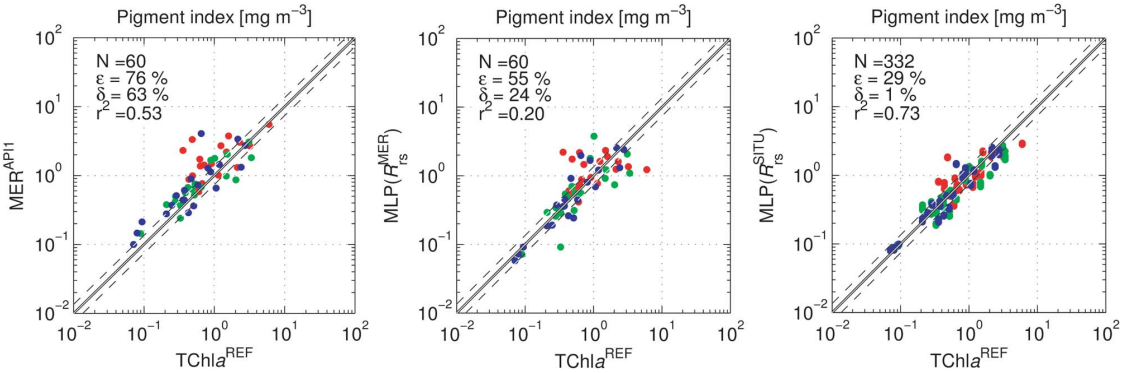

Fig. 1. Comparison with the TChla^{REF} of (a) standard MER^{API1} and equivalent products computed with regional algorithms, (b) MLP(R_{rs}^{MER}), and (c) MLP(R_{rs}^{SITU}), where the red, green, and blue dots correspond to stations A, B, and C, respectively.

TABLE I
COMPARISON BETWEEN STANDARD (MER$^{API\ 1}$), REGIONAL BIO-OPTICAL ALGORITHMS MLP(R_{rs}^{MER}) AND MLP(R_{rs}^{SITU}), AND TCHLa^{REF}

	N				ε(%)				δ(%)				r^2			
	SA	SB	SC	All	SA	SB	SC	All	SA	SB	SC	All	SA	SB	SC	All
MER$^{API\ 1}$ *vs* TChla^{REF}	19	20	21	60	118	44	69	76	104	27	55	63	0.55	0.66	0.42	0.53
MLP(R_{rs}^{MER}) *vs* TChla^{REF}	19	20	21	60	85	47	35	55	57	8	8	24	0.01	0.21	0.67	0.20
MLP(R_{rs}^{SITU}) *vs* TChla^{REF}	100	110	122	332	42	24	23	29	14	-9	0	1	0.62	0.85	0.79	0.73

B. Product Map Comparison

The comparison between the standard MERIS pigment index values and products derived with the regional MLP are presented in Fig. 2(a)–(f) and Table II. The distribution of pixels in shades of green in Fig. 2(b) corresponds to R_{rs} spectral values that are within the MLP(R_{rs}^{MER}) applicability range; shades of red indicate R_{rs} values outside this range. The regional MLP features a significant area of applicability in the MERIS image of the Atlantic off the Iberian Peninsula. As expected, zones out of the applicability range are mostly in clearer oceanic waters.

Three ROIs are identified in Fig. 2(e) to test the performance of the regional MLP in different areas along the coast of Portugal. These include the Figueira da Foz region influenced by the Mondego river plume (1 in red), the Lisbon region affected by the Tagus estuary (2 in green), and the Sagres region with minimal freshwater sources (3 in blue) and where the field data were collected for the development of the regional MLP.

The signed difference δ^* [Eq. (2)] between MERIS and regional products is presented in Fig. 2(d), where positive values indicate an overestimate by MER^{API1} with respect to MLP(R_{rs}^{MER}). Pixels where the relative difference between MER^{API1} and MLP(R_{rs}^{MER}) is less than -35% (underestimation) are colored in yellow. For the relative differences between -35% and 35%, the color is green. Finally, the overestimation by MERIS products with respect to regional MLP values more than 35% is marked in pink. Results derived from R_{rs} spectra within the MLP(R_{rs}^{MER}) applicability range are mostly between -35% and 35% [cf., Fig. 2(b) and (d)].

The scatter plot in Fig. 2(f) reports MER^{API1} *versus* MLP(R_{rs}^{MER}) data points by considering an ensemble of all ROI samples and by using the same color scheme adopted in Fig. 2(e). The statistical results are $\varepsilon^* = 37\%$ and $\delta^* = 36\%$, showing that there is a systematic difference between data products, with a high coefficient of determination (i.e., $r^2 = 0.88$). Statistical figures confirm the tendency toward overestimation by MER^{API1} in coastal regions shown also in Fig. 1 (red dots, station A).

Table II details the comparison between the MLP(R_{rs}^{MER}) and MER^{API1} at the three ROIs [i.e., results related to Fig. 2(f)]. Quantities labeled as N_{tot} and N_{val} indicate the total number of samples in each ROI before and after considering the MLP(R_{rs}^{MER}) applicability range as well as the MERIS product validity flags [4]. The number of retained samples is larger for the southern ROI, and the agreement between MER^{API1} and regional results improves with respect to the results for the northern and central ROI. This is in agreement with the development of the regional MLP algorithm using field measurements collected at the Sagres site.

The comparison between MER^{API1} and MLP(R_{rs}^{MER}) was expanded to consider MERIS satellite images between January 2008 and March 2012. Overall and seasonal statistical figures are summarized in Table III. Both products showed a similar pattern, where the values start to increase in spring, then attain higher values in summer followed by a slight decrease in autumn, and culminate in lower values in winter. It is also noted that a higher scattering and bias between the MER^{API1} and MLP(R_{rs}^{MER}) results occurred during the spring and summer months, with lower values occurring during the autumn and winter months. Over these years and in agreement with Fig. 2(f), the MLP(R_{rs}^{MER}) was generally lower than the MER^{API1}, especially during the summer months.

IV. DISCUSSION

This study reveals that differences between standard and regional API1 estimates vary among the sampling stations. Specifically, the quality of spaceborne data products improves

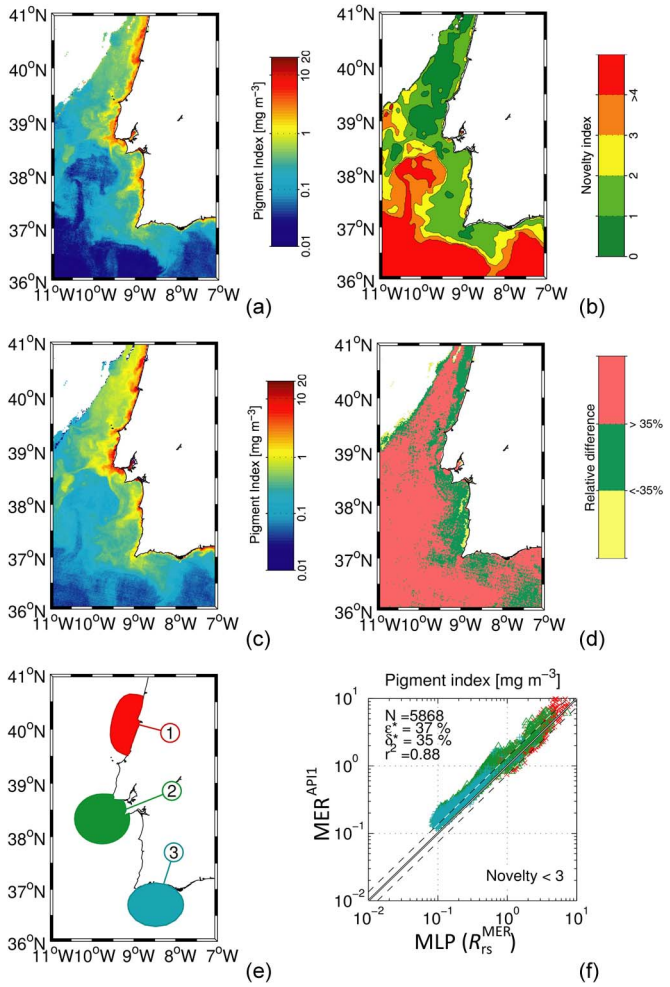

Fig. 2. Comparison between standard MERIS pigment index products and results obtained by applying the regional MLP for the Sagres region. (a) MLP($R_{\rm rs}^{\rm MER}$). (b) MLP applicability range. (c) MER$^{\rm API}$ RR Level 2 satellite image on August 25, 2010. (d) Relative percentage difference between MER$^{\rm API}$ and MLP($R_{\rm rs}^{\rm MER}$). (e) ROIs. (f) Scatter plots of MER$^{\rm API}$ *versus* MLP($R_{\rm rs}^{\rm MER}$).

TABLE II
COMPARISON BETWEEN THE STANDARD MER$^{\rm API1}$ AND THE REGIONAL MLP($R_{\rm rs}^{\rm MER}$) [FIG. 2(f)]

ROI	$N_{\rm tot}$	$N_{\rm val}$	ε*(%)	δ*(%)	r^2
#1	2122	2063	36.2	31.9	0.85
#2	3383	1653	39.1	38.5	0.90
#3	2946	2152	36.7	36.6	0.88
Total	8451	5868	37.2	35.5	0.88

when station A is excluded, particularly for MLP($R_{\rm rs}^{\rm MER}$), as documented in Fig. 1. This station is more affected by adjacency due to its proximity to the coast compared with stations B and C, as documented in earlier investigations [10].

The MLP($R_{\rm rs}^{\rm SITU}$) and the MLP($R_{\rm rs}^{\rm MER}$) have been tested with different combinations of input center wavelengths to derive the regional TChl*a* from $R_{\rm rs}$. The input set with the best performance includes $R_{\rm rs}$ at 490, 510, and 560 nm, while the blue (413 and 443 nm) and red (665 nm) wavelengths have been excluded to reduce degradation of the inversion performance. The $R_{\rm rs}$ values at 413, 443, and 665 nm tend to be less accurate due to limitations with the atmospheric correction scheme in the blue and red spectral regions [17]. Water leaving reflectances at 490, 510, and 560 nm also show less uncertainty and bias in a matchup analysis performed in the same study area for the comparison of MERIS with *in situ* radiometric data [9]. The need to select relevant input wavelengths for optimizing the performance of the regional algorithms to retrieve pigment indices has also been reported in other studies [4].

The matchup analysis (Fig. 1) and the comparison of product maps (Fig. 2) include evaluations of the standard product, regional estimates, and *in situ* TChl*a* measurements. The cross-checking of these results shows that the bias between MER$^{\rm API1}$ and TChl$a^{\rm REF}$ is 63%, whereas the bias between MLP($R_{\rm rs}^{\rm MER}$) and TChl$a^{\rm REF}$ is 24%. This concurs with the independent comparison of product maps indicating a bias of 36% between MER$^{\rm API1}$ and MLP($R_{\rm rs}^{\rm MER}$), i.e., close to the difference of the two former results. The convergence of these performance assessments supports the comparison of standard and regional maps of products as a means to analyze space mission deliverables, especially when the number of matchup data points is limited.

Investigations have focused specifically on the evaluation of the API1 product. Data analyses in selected ROIs indicate that this standard MERIS product tends to be higher than equivalent MLP estimates. This tendency to overestimation mostly features a systematic bias and reduced data scattering. A possible explanation could be systematic uncertainty deriving from the atmospheric correction process [9]. Another concurring reason could be an increase in yellow substances (YS) and/or nonalgal particles (NAP) in the study area with respect to case 1 waters with the same TChl*a* amount. Both YS and NAP tend to reduce $R_{\rm rs}$ values in the blue wavelengths. On the other hand, the NAP component induces a relatively uniform increase of $R_{\rm rs}$ in the visible domain. The composite effect of these factors could result in a higher spectral slope of $R_{\rm rs}$ in the blue-green spectral interval, causing the algorithm for API1 pigment index retrieval in case 1 waters to overestimate TChl*a* values.

The seasonal trend of the MER$^{\rm API1}$ and the MLP($R_{\rm rs}^{\rm MER}$) results has revealed that the higher values in the spring and summer months coincide with the upwelling season in the study area [5]. This phenomenon can explain the higher scattering and bias between the two data products during these seasons, when the variability is higher than in the autumn and winter. This preliminary time series analysis, documenting a seasonal component in the performance of standard API1 results, is supported by the accuracy of regional products evaluated with the reference *in situ* data.

A better understanding of relationships between optically active seawater compounds in the study area is necessary to progress with the present work. Sensitivity analyses are required to evaluate the effect of $R_{\rm rs}$ uncertainty budgets over the accuracy of higher order data products. These analyses should therefore be considered for future studies. Nevertheless, this present study demonstrates the importance of regression schemes that can efficiently use $R_{\rm rs}$ values at individual wavelengths, as in the regional MLP algorithms adopted here. Another outcome is the need to address the use of regional

TABLE III
COMPARISON OF THE STANDARD MER$^{\mathrm{API1}}$ AND THE REGIONAL MLP($R_{\mathrm{rs}}^{\mathrm{MER}}$) BETWEEN JANUARY 2008 AND MARCH 2012. THE SEASONS ARE DEFINED AS DECEMBER TO FEBRUARY FOR WINTER, MARCH TO MAY FOR SPRING, JUNE TO AUGUST FOR SUMMER, AND SEPTEMBER TO NOVEMBER FOR AUTUMN

	All		Winter		Spring		Summer		Autumn	
	MER$^{\mathrm{API1}}$	MLP($R_{\mathrm{rs}}^{\mathrm{MER}}$)	MER$^{\mathrm{API1}}$	MLP($R_{\mathrm{rs}}^{\mathrm{MER}}$)	MER$^{\mathrm{API1}}$	MLP($R_{\mathrm{rs}}^{\mathrm{MER}}$)	MER$^{\mathrm{API1}}$	MLP($R_{\mathrm{rs}}^{\mathrm{MER}}$)	MER$^{\mathrm{API1}}$	MLP($R_{\mathrm{rs}}^{\mathrm{MER}}$)
N	574		121		108		144		202	
Average	1.03	0.85	0.57	0.48	1.08	0.88	1.13	0.98	1.07	0.96
Max./Min.	11.10/0.07	8.37/0.02	2.25/0.19	2.64/0.19	6.53/0.11	4.52/0.05	8.09/0.11	3.63/0.08	11.10/0.07	8.37/0.02
ε* (%)	29.3		24.1		36.4		31.4		27.2	
δ* (%)	21.5		17.0		25.8		26.3		18.5	

algorithms for the Atlantic off Portugal by carefully considering their applicability range.

V. CONCLUSION

This letter has evaluated the standard MER$^{\mathrm{API1}}$ product, as well as the equivalent regional products MLP($R_{\mathrm{rs}}^{\mathrm{SITU}}$) and MLP($R_{\mathrm{rs}}^{\mathrm{MER}}$), with respect to reference *in situ* TChl*a* measurements in Sagres. The use of the regional MLP increases the accuracy of the data product, particularly during the upwelling season, when the higher concentrations of TChl*a* occur. It also shows a good applicability range not only in the study area but also in other regions off the Portuguese coast. The use of this regional algorithm can then complement standard algorithms designed for global applications. Furthermore, the testing of different input wavelengths to derive the regional TChl*a* from R_{rs} reveals the need to improve the atmospheric correction and reduce the larger R_{rs} uncertainties in the blue and red spectral regions.

This study also confirms the importance of maintaining the *in situ* measurement program at the reference sites, as well as the feasibility and relevance of using regional algorithms for timely evaluation of operational space mission deliverables as a cost-effective addition to the direct matchup analyses of primary radiometric data and derived bio-geophysical quantities. With this addition in mind, the methods adopted in this letter are also planned to support the analysis of the forthcoming Sentinel-3/OLCI data products. Additional applications in the near future include aquaculture management and the implementation of European Union directives for coastal and marine areas.

ACKNOWLEDGMENT

The authors would like to thank the two external reviewers for their sound advice on improvements to this letter.

REFERENCES

[1] C. Donlon *et al.*, "The Global Monitoring for Environment and Security (GMES) Sentinel-3 mission," *Remote Sens. Environ.*, vol. 120, pp. 37–57, Feb. 2012.

[2] "Regulation (EU) no 377/2014 of the European Parliament and of the Council of 3 April 2014 Establishing the Copernicus Programme and Repealing Regulation (EU) no 911/2010," Eur. Regulation, Vienne, France, 2014.

[3] A. Morel and D. Antoine, "Pigment Index Retrieval in Case 1 Waters," Laboratoire d'Océanographie de Villefranche, Villefranche-sur-Mer Cedex, France, Algorithm Theoretical Basis Document PO-TN-MEL-GS-0005, Jan. 2007.

[4] T. Kajiyama, D. D'Alimonte, and G. Zibordi, "Regional algorithms for European seas: A case study based on MERIS data," *IEEE Geosci. Remote Sens. Lett.*, vol. 10, no. 2, pp. 283–287, Mar. 2013.

[5] S. Loureiro, A. Newton, and J. D. Icely, "Microplankton composition, production and upwelling dynamics in Sagres (SW Portugal) during the summer of 2001," *Sci. Mar.*, vol. 69, no. 3, pp. 323–341, Jan. 2005.

[6] G. Zibordi, F. Mélin, J.-F. Berthon, and E. Canuti, "Assessment of MERIS ocean color data products for European seas," *Ocean Sci. Discuss.*, vol. 10, no. 1, pp. 219–259, Jan. 2013.

[7] D. Antoine *et al.*, "Assessment of uncertainty in the ocean reflectance determined by three satellite ocean color sensors (MERIS, SeaWiFS and MODIS-A) at an offshore site in the Mediterranean Sea (BOUSSOLE project)," *J. Geophys. Res., Oceans*, vol. 113, Jul. 2008, Art. no. C07013.

[8] S. Cristina, P. Goela, J. D. Icely, A. Newton, and B. Fragoso, "Assessment of water-leaving reflectances of oceanic and coastal waters using MERIS satellite products off the Southwest Coast of Portugal," *J. Coastal Res.*, vol. SI 56, pp. 1479–1483, Dec. 2009.

[9] S. Cristina, G. F. Moore, P. C. Goela, J. D. Icely, and A. Newton, "*In situ* validation of MERIS marine reflectance off the southwest Iberian Peninsula: Assessment of vicarious adjustment and corrections for near-land adjacency," *Int. J. Remote Sens.*, vol. 35, no. 6, pp. 2347–2377, Mar. 2014.

[10] S. Cristina, J. Icely, P. C. Goela, T. A. DelValls, and A. Newton, "Using remote sensing as a support to the implementation of the European marine strategy framework directive in SW Portugal," *Continental Shelf Res.*, vol. 108, pp.169–177, Oct. 2015.

[11] S. Wright and S. Jeffrey, "High-resolution HPLC system for chlorophylls and carotenoids of marine phytoplankton," in *Phytoplankton Pigments in Oceanography*. Paris, France: UNESCO, 1997, pp. 327–341.

[12] P. Goela *et al.*, "Using CHEMTAX to evaluate seasonal and interannual dynamics of the phytoplankton community off the South-west Coast of Portugal," *Estuarine, Coastal Shelf Sci.*, vol. 151, pp. 112–123, Oct. 2014.

[13] D. D'Alimonte, G. Zibordi, T. Kajiyama, and J.-F. Berthon, "Comparison between MERIS and regional high-level products in European seas," *Remote Sens. Environ.*, vol. 140, pp. 378–395, Jan. 2014.

[14] C. M. Bishop, "Novelty detection and neural network validation," *Proc. Inst. Elect. Eng.—Vis. Image Signal Process.*, vol. 141, no. 4, pp. 217–222, Aug. 1994.

[15] D. D'Alimonte, F. Mélin, G. Zibordi, and J.-F. Berthon, "Use of the novelty detection technique to identify the range of applicability of empirical ocean color algorithms," *IEEE Trans. Geosci. Remote Sens.*, vol. 41, no. 12, pp. 2833–2843, Dec. 2003.

[16] F. Mélin *et al.*, "Multi-sensor satellite time series of optical properties and chlorophyll-a concentration in the Adriatic Sea," *Prog. Oceanogr.*, vol. 91, no. 3, pp. 229–244, Nov. 2011.

[17] T. Cui *et al.*, "Assessment of satellite ocean color products of MERIS, MODIS and SeaWiFS along the East China Coast (in the Yellow Sea and East China Sea)," *ISPRS J. Photogramm.*, vol. 87, pp. 137–151, Jan. 2014.